Polarization Gratings for Visible and Near-Infrared Astronomy

Max Millar-Blanchaer[a], Dae-Sik Moon[a], James R. Graham[b] and Micheal Escuti[c]

[a]University of Toronto, Dept. of Astronomy, Toronto ON M5S 3H4, Canada;
[b]UC Berkeley, Dept. of Astronomy, Berkeley CA 94720, United States;
[c]North Carolina State University, Dept. of Electrical & Computer Engineering, Raleigh, NC 27695-7914, USA

ABSTRACT

We report on the development of polarization gratings that can be used for polarimetry and/or high throughput broadband spectroscopy in astronomy. Polarization gratings are able to overcome fundamental limitations on the diffraction efficiency of conventional gratings to provide near 100% diffraction efficiency over a broad bandwidth. The broad spectral coverage of these devices will be useful for observations of gamma-ray bursts and supernovae of unknown the redshift, where spectral features may fall over a range of wavelengths. As a spectropolarimeter a polarization grating would be ideal, for example, for the study of dusts and hazes, whose polarimetric properties vary with wavelength. We present the results of a series of laboratory measurements of the diffraction efficiency and modulation efficiency of a prototype grating designed for operation from 500 to 900 nm. We find that the grating is able to achieve greater than 90% diffraction efficiency from 500 to 850 nm and modulate incident circular polarized light with an efficiency of $\sim$ 99%. Our future plans include on-sky testing at a small local telescope, with an eventual goal of incorporating a polarization grating into the design of a microshutter array-based multi-object visible/NIR spectrograph for a 10m class facility.

Keywords: Polarization gratings, spectropolarimetry, broadband spectroscopy, polarimetry, instrumentation

1. INTRODUCTION

A polarization grating[1–4] is a type of diffraction grating that can be designed to diffract incident light with high efficiency into only the $m = +1$ and/or $m = -1$ orders. The amount of light diffracted into each order depends on the circular polarization state of the incoming beam, so that they act simultaneously as polarization beam splitters and spectrally dispersive gratings. In contrast to conventional surface relief gratings, which affect the phases of orthogonal polarizations equally, polarization gratings (PGs) are able to control the two phases separately. As a result, PGs can readily overcome the fundamental limitations on the diffraction efficiency of ruled gratings.[5] Conventional gratings may be blazed to achieve relatively high diffraction efficiencies, but only over a small wavelength range. In these cases diffraction efficiency must often be traded for a spectral coverage. PGs, on the other hand, are able to achieve near perfect diffraction efficiency over a near unity bandwidth, $\Delta\lambda/\lambda_0 \approx 1$.[6,7] This highly desirable property makes PGs relevant as dispersing elements not only for polarimetric applications, but for normal spectroscopy as well.

The development of these devices has been spearheaded by one of the co-authors of this work at North Carolina State University, where the applications to date have mostly been in display, telecommunications, beam steering, and remote sensing fields. PGs have been previously considered by Pakhham et al. (2010)[4] for mid infrared spectropolarimetry for SOFIA and later this fall a PG is expected to be installed as an instrument upgrade to MMT-POL.[8,9] Whereas these two efforts have mostly involved using PGs in the IR, our work focuses on using PGs in the visible and near infrared (NIR).

Our eventual goal is to develop a PG that operates from 600 to 1600 nm that can be included in a spectropolarimeter on a large telescope. As a first step we have designed and fabricated a set of PGs that have been

Further author information: (Send correspondence to M.M.-B.)
M.M.-B.: E-mail: maxmb@astro.utoronto.ca, Telephone: 1 416 946 5243

Advances in Optical and Mechanical Technologies for Telescopes and Instrumentation, edited by Ramón Navarro, Colin R. Cunningham, Allison A. Barto, Proc. of SPIE Vol. 9151, 91514I
 doi: 10.1117/12.2056998

optimized for near unity diffraction efficiency between 500 and 900 nm. Here we present the results of diffraction efficiency and modulation efficiency measurements carried out at the University of Toronto on one of the gratings. Following further lab tests the grating will be included in the design of a simple visible spectropolarimeter for a small local telescope.

In § 2 we summarize the basic properties of polarization gratings and provide a description of our visible PGs. A description of our lab test set-up and our laboratory measurements can be found in § 3. In § 4 we consider science targets for PGs in the visible and NIR regimes and explore several possible instrument architectures. Our future plans are discussed in § 5.

2. POLARIZATION GRATINGS

The PGs developed at NCSU are based on liquid crystal polymer thin film coatings, which take advantage of the Pancharatnam-Berry effect to induce a phase delay on incident light. A simple PG can be made with uniaxially birefringent liquid crystals that rotate in one direction along the grating surface. By designing the thin film to induce a half-wave of retardance for a central wavelength, it can be shown (e.g. McManamon et al. 2009[10]) that a change in orientation from 0 to π in liquid crystal orientation can impart a phase delay of 0 to 2π to on-axis light. By regularly repeating a 180° rotation across the grating plane, one can construct a PG that follows standard diffraction theory, where a 180° rotation defines the grating period. In particular, the periodic pattern causes PGs to diffract light as a function of wavelength following the grating equation. The 2π phase delay has the effect of sending light into only the $m = +1$ and/or $m = -1$ orders at a very high efficiency.

The birefringence of the liquid crystals creates a sensitivity to the circular polarization state of the incident light, which as a result sends purely left-hand circular or right-hand circular polarized light exclusively to the $m = +1$ or $m = -1$ order, respectively. Unpolarized and linearly polarized light is diffracted equally between the two orders. Regardless of the incident polarization, the total intensity can be recovered by summing the $m = +1$ and $m = -1$ orders.

This design is able to deliver near unity diffraction efficiency (when you sum the $m = +1$ and $m = -1$ orders), but only at the central wavelength, where the thickness of the thin film induces a half-wave of retardance. The wavelength coverage can be extended by sandwiching together two polarization gratings, each with a chiral nematic twist of opposite handedness induced in the liquid crystals along the direction of the optical axis. For a two layer grating the diffraction efficiency can be shown to be:

$$\eta_{\pm 1} = A(\frac{1 \mp V}{2})(\cos^2 X + \Phi^2 \,\mathrm{sinc}^{\,2} X) \tag{1}$$

where V is Stokes V, $X = \sqrt{\Phi^2 + \Gamma^2}$, $\Gamma = \pi \Delta n d/\lambda$, and $A = 2\Gamma sinc X$ (see Oh and Escuti 2007[6] for derivation). These equations are governed by the thin film properties: Δn is the birefringence of the liquid crystals, d is the thickness of the file and Φ is the total rotation of the liquid crystals along the optical axis of each layer. By optimizing these three parameters, the grating can be designed to have a diffraction efficiency above 99% over a bandwidth $\Delta\lambda/\lambda_0 \sim 0.57$. In reality manufacturing defects can result in slightly lower performance, but very high diffraction efficiency is still achievable at some wavelengths (see § 3 for lab results). The sensitivity to circular polarization can be seen explicitly in this equation, where the difference of the two orders is directly proportional to Stokes V.

The bandwidth coverage can be extended even further to $\Delta\lambda/\lambda_0 \sim 1$ by using three layers of liquid crystal, each with their own twist.[11] Our work concerns this three layer design, where the extended wavelength coverage will be useful for extending the wavelength coverage into the near infrared.

Parameter	Value
Central Wavelength, λ_0	700 nm
Diffraction Efficiency Range	$500 - 900$ nm
Grating Period	5 μm
Grating Diameter	20 mm

Table 1. The design parameters for the PGs designed for testing at the University of Toronto.

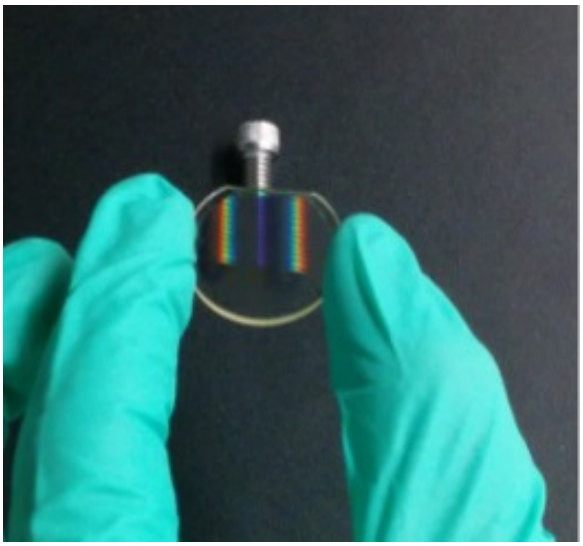

Figure 1. A photo of a visible PG, designed for testing at the University of Toronto. Where the PG is placed above the screw, images appear in the $m = +1$ and $m = -1$ orders. At bluer wavelengths the efficiency is not as high and the zeroth order can be seen at the center of the grating.

With the eventual goal of producing a grating that can operate in both the visible and NIR in mind, we decided to first work with a three layer prototype grating designed only for the visible regime. Narrowband PGs have been produced for beam steering applications in the NIR,[12,13] but broadband PGs covering 600 to 1600 nm require additional design work. Visible PGs, on the other hand, have already been produced at NCSU[14] and the subtleties of their fabrication are well understood. In addition, working in visible wavelengths is simpler from an instrument testing point of view: you can use relatively cheap silicon detectors and no cryogenics are needed.

A set of four prototype polarization gratings with identical design parameters have been designed and fabricated for near unity throughput from 500 to 900 nm (see Table 1). The clear aperture is 18-20 mm and the grating period is 5 μm. These gratings will be used for laboratory characterization (see § 3) and in future astronomical instruments for broadband spectroscopy and spectropolarimetry (see § 5). In this paper we focus on the analysis of just one of the four gratings, pictured in Figure 1.

3. LABORATORY CHARACTERIZATION

The main goal of these lab tests is to characterize the diffraction efficiency and the modulation efficiency of the prototype gratings. Here we define the diffraction efficiency as the fraction of the total flux leaving the PG, that gets dispersed into the $m = +1$ and $m = -1$ orders at a given wavelength. The modulation efficiency is the amplitude of the flux difference between the $m = +1$ and $m = -1$ orders normalized by their sum as the incident polarization is modulated from $V = +1$ to $V = -1$. The normalized flux difference is equal to the fractional circular polarization seen by the PG. A large modulation efficiency is required for the measurements of faint polarization signals in noisy conditions. With these two measurements in mind, the lab set-up has been designed to relay light from a broadband source through a set of optional polarizing optics to the polarization grating, and then focus the $m = -1$, $m = 0$ and $m = 1$ orders onto a detector.

3.1 Lab Set-up

The lab set-up is depicted in Figure 2. Light from a tungsten lightbulb enters the fiber via a fiber collimation package (not pictured). The collimation package helps to focus the light onto the fiber tip and greatly increases the collecting area of the fiber. Using the fiber allows us to separate our light source from the rest of the optical system, significantly reducing the scattered light in the system and the output of the fiber acts as a point source on the focal plane. The light exits the fiber and is then formed into a $\sim$20 mm diameter beam by a collimating

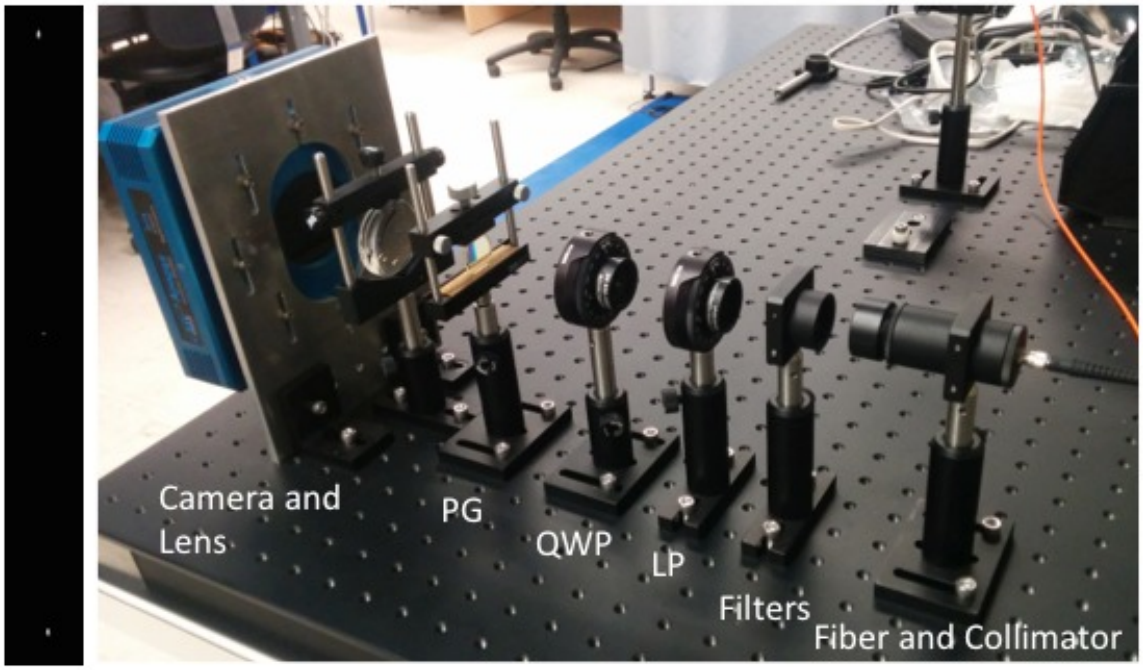

Figure 2. *Left* - An example of the raw detect image from our lab set-up with the 900nm filter in the beam. The first two orders, which are slightly extended due to the 10 nm FWHM bandwidth of the interference filters, can be seen at the top and bottom sides of the image, with the zeroth order in the center. *Right* - Our laboratory test set-up, from right to light (following the path of the light): optical fiber, collimating lens, filter set, LP, QWP, PG, cameral lens, Apogee F16M camera. The set-up is able to produce circular polarized light from Stokes $V = +1$ to $V = -1$, and focus all three orders on the detector across the visible regime.

lens, after which it passes through a series of removable filters and polarizing optics. The filters include both Neutral Density filters, to control the total intensity reaching the detector, and bandpass interference filters with central wavelengths spaced every 50 nm from 400 to 900 nm (10 nm FWHM).

A Thorlabs LPVIS100-MP2 thin-film nanoparticle polarizer can be placed into the beam to generate linearly polarized light, which is then converted to circular polarized light by the Thorlabs AQWP10M-980 Achromatic Quarter Waveplate. Both components were mounted in manual rotation stages, where 0° corresponds to the polarization axis and the fast axis of the LP and QWP, respectively, being vertical in the lab reference frame. The combination of these two components allows for the full exploration of the surface of the Poincaré sphere. Assuming ideal polarizing components, with the LP fixed at 0° the Stokes V reaching the PG is equal to $\sin(2\psi)$, where ψ is the position angle of the QWP read off the rotation stage. In reality, the QWP only delivers a quarter-wave retardance from 690 to 1200 nm, and so the above equation is only valid in that range. Thus we focus our polarization analysis on the wavelengths from 700 to 900 nm, where the set-up is able to generate Stokes V from $V = +1$ to $V = -1$.

After the LP and QWP, the collimated light beam passes through the PG and is focused on to the detector by an F/1.5 camera lens. The detector is an Apogee F16M camera, a 4096x4096 pixel array of 9 μm pixels. The large surface area of the detector (3.68cm x 3.68cm) allows both of the first diffraction orders and the zeroth order to be measured simultaneously across our entire wavelength range (see Figure 2).

3.2 Lab Measurements

Diffraction efficiency measurements were made with one bandpass filter in place at a time and both the LP and QWP out of the beam. The diffraction efficiency at each wavelength, $\eta_{\Sigma\pm1}$, was calculated as:

$$\eta_{\Sigma\pm1}(\lambda) = \frac{\sum_{m=\pm1} F_m(\lambda)}{\sum_{m=-1,0,1} F_m(\lambda)} \tag{2}$$

where $F_m(\lambda)$ was the flux measured in the mth order when the bandpass filter of central wavelength λ was in the beam. For these calculations the light diffracted into higher orders is assumed to be negligible compared to the zero order leakage, which has yet to be experimentally confirmed here, but has been the case for previous visible PGs.[14] The overall transmittance of the grating (i.e. F_{out}/F_{in}) will be a combination of the reflectance, absorption and diffraction efficiency. The thin-film grating itself has negligible absorption and the absorption of the substrate will depend on the choice of glass. The reflectance can be controlled with an anti-reflection coating. In our case we expect both the absorption and reflectance to be very low and so the transmittance and diffraction efficiency should be very similar.

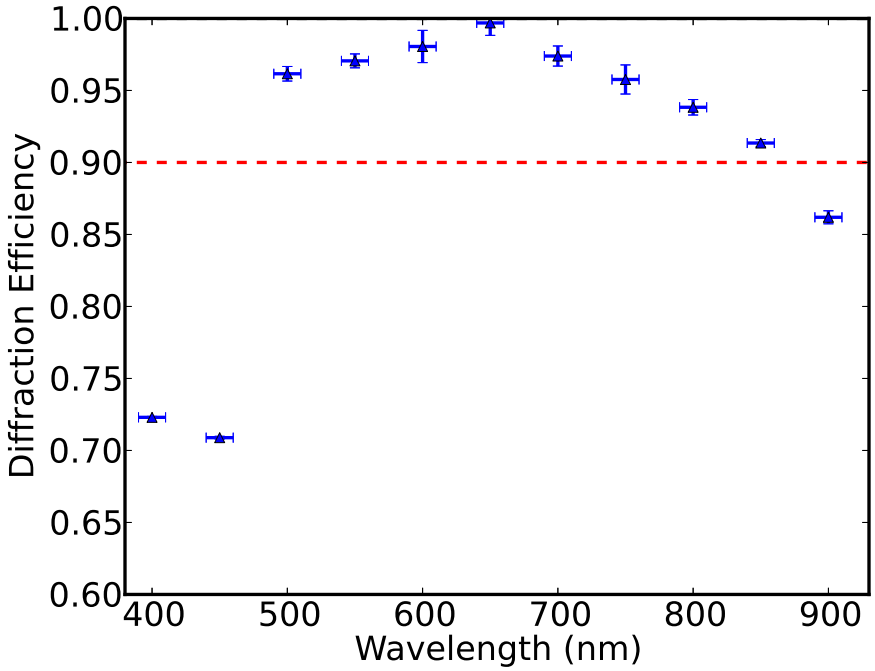

Figure 3. The diffraction efficiency of the visible PG. The red dashed line indicates 90% diffraction efficiency. The error bars in the wavelength direction represent the 10nm FWHM of the bandpass filters. A peak efficiency of 99.7% is achieved at 650nm.

The measured diffraction efficiency from 400 to 900 nm can be see in Figure 3. The camera lens was found to create a small amount of coma in the spots produced in the $m = +1$ and $m = -1$ orders. We measured the flux in each spot using aperture photometry, with apertures large enough to contain the central spots, but not necessarily the entire coma. As a consequence, the flux measurements are likely underestimated for the two first order spots, which in turn would underestimate the diffraction efficiency calculation. However, the effect is likely small since most of the flux is concentrated in the central spot. We find that the PG is able to produce a diffraction efficiency of greater than 90% between 500 and 850 nm, with a peak of 99.7% at 650 nm. At 900 nm the diffraction efficiency was measured to be 86.2%. These results indicate that the polarization grating can achieve high diffraction efficiency across a large bandwidth, as expected.

The fractional circular polarization measured by the PG, P_{frac}, has been be calculated as:

$$P_{frac} = \frac{F_1(\psi) - F_{-1}(\psi)}{F_1\psi + F_{-1}(\psi)} \tag{3}$$

where $F_m(\psi)$ was the flux measured in the mth order when the QWP was at an angle of ψ. The measurements of the circular polarization fraction with the QWP at position angles from 0 to 180 can be found in Figure 3. From Equation 1, the circular polarized fraction is expected to follow the incident circular polarization state, i.e. Stokes V=$\sin(2\psi)$. A sinusoidal pattern is recovered at all wavelengths, with high levels of modulation across

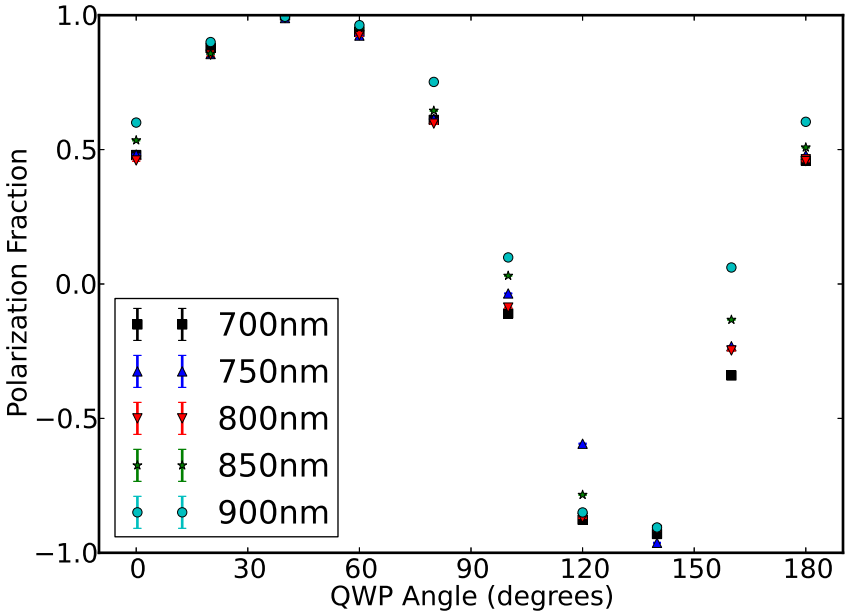

Figure 4. The modulation efficiency of the PG from 700 to 900 nm, measured every 20°. A peak modulation efficiency of 99.9% is reached at 700 nm.

the entire range. The shape of the polarization fraction curve in Figure 3 appears to be slightly distorted from a perfect sinusoid: between 0° and 90° the shape appears wider than expected and between 90° and 180° it is narrower. This discrepancy is possibly due to either a measurement error or misaligned optics, as previous PG studies have reproduced the expected curve with much higher fidelity.[2]

The modulation efficiency could be measured either directly by measuring the maximum and minimum polarization fractions, which should occur at 45° and 135°, or by fitting a sine curve to the data. Because of the poor fit to a sine curve, and the lack of appropriate measurements neither of these methods are possible. Instead we consider the modulation efficiency to be the maximum absolute value measured, which should provide a lower limit on the actual modulation efficiency. The polarization fraction reaches a peak polarized fraction of 99.9% at 700nm, and all wavelengths peak above 98%. Thus, regardless of the exact shape of the curve in Figure 4, the fact that modulation efficiencies of ∼99% are reached indicates the PG is indeed an efficient polarization beam splitter.

4. SCIENTIFIC APPLICATION OF POLARIZATION GRATINGS

The broad high-throughput spectral coverage of PGs will be very useful for conducting observations of diverse types of astronomical objects, especially those objects that can benefit significantly by broadband medium-resolution spectroscopic information. Any objects of unknown nature, e.g., previously-unknown objects discovered in a new survey or in a serendipitous manner, or of unknown redshift naturally belong to the group. For this type of objects, coarse broadband information is more urgent and can pave the way to more detailed observations to understand their nature and redshift. Due to the recent rapid development in the detector technology, now it is possible to have a large format (e.g., 2K x 2K number of pixels) detector array that has high quantum efficiencies in a broad wavelength range in the visible-NIR regime such as the substrate-removed HgCdTe Hawaii II RG (H2RG) array that has 60% quantum efficiency not only in the NIR but also over a significant portion of the visible waveband. We are particularly interested in the PG-based visible-NIR spectroscopy simultaneously covering the 0.6-1.6 micron range at R $\sim$ 1,000 spectral resolving power using an H2RG for observations of gamma-ray bursts and/or supernovae of high-redshift or unknown redshift. Polarization gratings will also

be very useful in measuring the polarization state of astronomical objects, such as dust and haze in planetary systems and exoplanet atmospheres whose polarimetric properties vary with wavelength.[15]

4.1 Polarization Grating based spectrograph designs

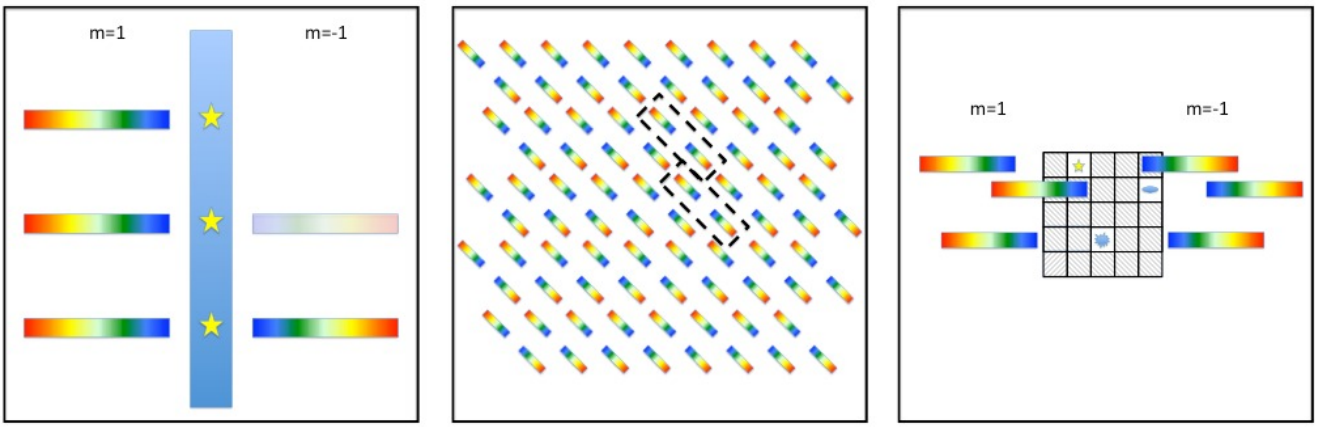

Figure 5. *Left* - An example of three different spectra dispersed by a PG in a long slit spectrograph. The top source is completely polarized and so only the $m = +1$ order is visible. The middle source is partially polarized and so the the $m = -1$ order is visible, but with a lower intensity. The bottom source is randomly polarized and so both $m = +1$ and $m = -1$ orders are visible with equal intensity. *Center* - The focal plane of a lenslet array based integral field spectrograph equipped with a PG. When viewing an extended source each lenslet produces a pair of spectra (dashed black line), which allows for spectropolarimetry at each spatial location. *Right* - The focal plane of a microshutter array-based spectropolarimeter using a PG.[16] A microshutter array picks off sources from the FOV which each produce a pair of spectra on the focal plane.

Since PGs function as diffraction gratings, one could imagine including them in most of the standard spectrograph architectures seen in modern instruments. A simple slit-based dual-channel spectropolarimeter could be constructed with a quarterwave-plate (QWP) as a modulator and a PG as an analyzer. The design would follow the basic design of a spectrograph, but with the inclusion of a QWP in the collimated beam, to convert incident linear polarized light to circular polarized light . Figure 5 depicts the focal plane arrangement for a slit-based spectropolariemter as well as two other possible design schemes of a PG-based spectrograph: an integral field spectrograph and a multi-object spectrograph. Each of the three implementations could be used both as a normal spectrograph, by summing the two dispersion orders, or as a spectropolarimeter, by taking the difference of the two orders at different QWP rotation angles.

5. FUTURE PLANS AND CONCLUSIONS

The unexpected shape of Figure 3 curve clearly shows that a deeper understanding of the lab measurements is required. While this is likely due to measurement error, if it isn't then the behaviour must be fully understood before including the PG in an instrument. In addition we wish to characterize the modulation behaviour of the PG from 500 to 700 nm to fully understand the polarimetric behaviour of the PG.

Following the lab tests we plan to design and build a proof-of-concept visible slit-based spectropolarimeter with the prototype grating to be tested on the 16" University of Toronto campus telescope. We will use such an instrument to measure the polarization of highly polarized stars and of polarized solar system objects. Assuming satisfactory on-sky results we plan to bring the visible spectropolarimeter to a larger telescope. In conjunction with these efforts, we plan to design and test a PG that extends the wavelength coverage into the NIR: with high diffraction efficiency from 600 to 1600 nm. This grating will then be included in a microshutter array-based multi-object spectrograph currently under development at the University of Toronto.[16]

In conclusion, polarization gratings are a unique new technology that have many potential applications in astronomy. Their broadband diffraction efficiency is unmatched by other gratings and their polarimetric capabilities allow for broadband spectropolarimetry. Our laboratory tests indicate that high diffraction efficiencies ($> 90\%$) are achievable across large bandwidths, with extremely high efficiencies ($> 99\%$) at some wavelengths. Modulation efficiencies on the order of $\sim 99\%$ mean that the PGs are very effective polarization beam splitters. In the very near future these devices will be on-sky providing many new and exciting scientific developments.

ACKNOWLEDGMENTS

This research has been supported by the Leaders Edge Fund of the Canadian Foundation for Innovation and Large Infrastructure program of the Ontario provincial government in Canada. MJE gratefully acknowledges the support of the National Science Foundation (NSF grant ECCS-0955127, PECASE).

REFERENCES

[1] Crawford, G. P., Eakin, J. N., Radcliffe, M. D., Callan-Jones, A., and Pelcovits, R. A., "Liquid-crystal diffraction gratings using polarization holography alignment techniques," *Journal of Applied Physics* **98**, 123102–123102–10 (Dec 2005).

[2] Escuti, M. J., Oh, C., Snchez, C., Bastiaansen, C., and Broer, D. J., "Simplified spectropolarimetry using reactive mesogen polarization gratings," *Proc. SPIE* **6302**, 630207–630207–11 (2006).

[3] Provenzano, C., Pagliusi, P., and Cipparrone, G., "Highly efficient liquid crystal based diffraction grating induced by polarization holograms at the aligning surfaces," *Applied Physics Letters* **89**(12), – (2006).

[4] Packham, C., Escuti, M., Ginn, J., Oh, C., Quijano, I., and Boreman, G., "Polarization Gratings: A Novel Polarimetric Component for Astronomical Instruments," *PASP* **122**, 1471–1482 (Dec. 2010).

[5] Wyrowski, F., "Upper bound of the diffraction efficiency of diffractive phase elements," *Opt. Lett.* **16**, 1915–1917 (Dec 1991).

[6] Oh, C. and Escuti, M. J., "Achromatic polarization gratings as highly efficient thin-film polarizing beam-splitters for broadband light," *Proc. SPIE* **6682**, 668211–668211–12 (2007).

[7] Escuti, M. and Oh, C., "Multi-layer achromatic liquid crystal polarization gratings and related fabrication methods," (Sept. 9 2010). US Patent App. 12/596,176.

[8] Packham, C. Private Communications.

[9] Packham, C., Jones, T. J., Warner, C., Krejny, M., Shenoy, D., Vonderharr, T., Lopez-Rodriguez, E., and DeWahl, K., "Commissioning results of mmt-pol: the 1-5um imaging polarimeter leveraged from the ao secondary of the 6.5m mmt," *Proc. SPIE* **8446**, 84463R–84463R–12 (2012).

[10] McManamon, P. F., Bos, P. J., Escuti, M., Heikenfeld, J., Serati, S., Xie, H., and Watson, E., "A review of phased array steering for narrow-band electrooptical systems," *Proceedings of the IEEE* **97**, 1078–1096 (June 2009).

[11] Komanduri, R. K., Lawler, K. F., and Escuti, M. J., "Multi-twist retarders: broadband retardation control using self-aligning reactive liquid crystal layers," *Opt. Express* **21**, 404–420 (Jan 2013).

[12] Oh, C., Kim, J., Muth, J., Serati, S., and Escuti, M., "High-throughput continuous beam steering using rotating polarization gratings," *Photonics Technology Letters, IEEE* **22**, 200–202 (Feb 2010).

[13] Kim, J., Oh, C., Serati, S., and Escuti, M. J., "Wide-angle, nonmechanical beam steering with high throughput utilizing polarization gratings," *Appl. Opt.* **50**, 2636–2639 (Jun 2011).

[14] Oh, C. and Escuti, M. J., "Achromatic diffraction from polarization gratings with high efficiency," *Opt. Lett.* **33**, 2287–2289 (Oct 2008).

[15] Stam, D. M., Hovenier, J. W., and Waters, L. B. F. M., "Using polarimetry to detect and characterize Jupiter-like extrasolar planets," A&A **428**, 663–672 (Dec. 2004).

[16] Moon, D.-S., Sivanandam, S., Kutyrev, A. S., Jr., S. H. M., and Graham, J. R., "The development of ground-based infrared multi-object spectrograph based on the microshutter array," *Society of Photo-Optical Instrumentation Engineers (SPIE) Conference Series* **9147** (2014).